Iterative phase recovery using wavelet domain constraints

Leili Baghaei,[a] Ali Rad, Bing Dai, Piero Pianetta, and R. Fabian W. Pease
Department of Electrical Engineering, Stanford University, Stanford, California 94305

Jianwei Miao
Department of Physics and Astronomy and California NanoSystems Institute, University of California, Los Angeles, California 90095

(Received 10 July 2009; accepted 12 October 2009; published 7 December 2009)

Phase retrieval is a central problem in coherent x-ray diffraction microscopy. Various methods have been proposed to solve the problem with the most successful being iterative methods with a finite spatial support constraint. In this work, a new constraint is formulated in the wavelet domain using low-resolution *a priori* information. Experimental results indicate that the constraint is sufficient to reconstruct an object from Fourier modulus measurements. © *2009 American Vacuum Society.*
[DOI: 10.1116/1.3258632]

I. INTRODUCTION

Coherent x-ray diffraction microscopy is gaining attention as a potential high-resolution microscopy tool for two-dimensional (2D) and three-dimensional imaging. One of the fundamental issues in diffraction microscopy is that the measurements obtained are of the Fourier modulus only. Some form of phase retrieval is necessary to combine with the Fourier modulus data to allow a reconstruction.[1–4]

The phase retrieval problem can be formulated as a constraint satisfaction problem. A solution is sought, which simultaneously satisfies a number of constraints. These constraints can be expressed as sets and so a feasible solution is one (of possibly many) which lies in the intersection of the constraint sets, as seen in Fig. 1. If the constraint sets are large and the intersection is nontrivial, then finding a solution can be difficult.

The difference map algorithm is an iterative projection based method for constraint satisfaction problems.[5] For two constraint sets, A and B, the algorithm requires projection operators, P_A and P_B. Briefly, a projection operator is a transformation from a vector space to itself with the property that the image is unchanged under a second projection, i.e., $P^2 = P$. In this context, the projection takes a point outside the constraint set and projects it to a point within the set. In many cases (but not all), the projection is an *orthogonal* projection where the image is the closest point in the set. From an initial guess, the algorithm computes the next and subsequent iterate as follows:

$$x \to D(x) = x + \beta[P_A(f_B(x)) - P_B(f_A(x))], \tag{1}$$

$$f_A(x) = P_A(x) - \frac{1}{\beta}(P_A(x) - x), \tag{2}$$

$$f_B(x) = P_B(x) + \frac{1}{\beta}(P_B(x) - x). \tag{3}$$

[a]Electronic mail: leili@stanford.edu

The real parameter β can be of either sign with the optimal value dependent on the application and determined through experimentation. For $\beta = 1$ (or -1), the mapping simplifies to

$$D(x) = x + P_A(2P_B(x) - x) - P_B(x), \tag{4}$$

which is seen to be of the same form as Fienup's hybrid input-output (HIO) algorithm[1] and thus can be seen as a generalization. The progress can be monitored by inspecting the norm of the difference of the two projections

$$\Delta = |P_A(f_B(x)) - P_B(f_A(x))|. \tag{5}$$

When Δ vanishes, a fixed point has been found which satisfies both constraint sets and the algorithm is terminated. The uniqueness of the solution is not guaranteed since the size of the solution space is not necessarily restricted to a single point.

In the phase retrieval problem the solution is constrained to have Fourier modulus *close* to the known or measured values modulus values. The interpretation of close depends on the application, in some cases it may mean *exact* but usually, due to noise, it will mean within some bounds or interpreted probabilistically. For simplicity, we will assume exact, giving the constraint set

$$A = \{x \| |\mathcal{F}(x)| = X_F^{\text{meas}}\}, \tag{6}$$

that is, all real space images, x, which have their Fourier modulus equal to the known measured values, X_F^{meas}. For this set, the *orthogonal* projection is formed by first transforming to Fourier space, then, for each coefficient, replacing the magnitude with the known value before inverse transforming. This corresponds to projecting each Fourier coefficient on the complex plane to the nearest point on the circle of radius of the known value

$$P_A(x) = \mathcal{F}^{-1}(X_F^{\text{meas}} e^{iX_p}), \tag{7}$$

$$X_p = \angle \mathcal{F}(x). \tag{8}$$

The second constraint set is often taken as a finite spatial support constraint.[1,6] This constraint requires that the sample

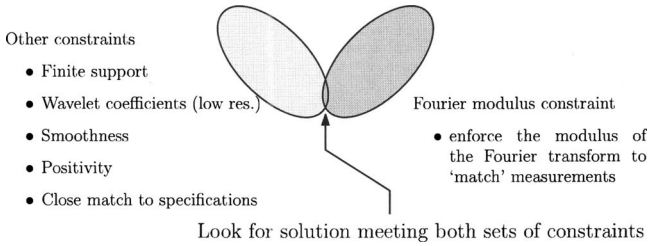

FIG. 1. General phase retrieval constraint problem. The known information forms two constraint sets, and a solution is sought, which simultaneously satisfies both sets. One constraint set enforces the measured Fourier modulus values. The other constraint set can be formed from different forms of *a priori* information. For example, this might be knowledge on the spatial support of the object or a low-resolution image of the object.

values be zero for all points in some region. If the support is denoted by the indicator $\mathbf{1}_S$, then the constraint set B is given as

$$B = \{x | x(\mathbf{1}_S = 0) = 0\} \tag{9}$$

and the *orthogonal* projection is simply

$$P_B(x) = \mathbf{1}_S \cdot x, \tag{10}$$

where, for each point outside the support, the value is set to zero.

Since the Fourier modulus information does not sufficiently constrain the problem, it is necessary for the second constraint space to provide enough additional information to allow the solution to be found. In Ref. 7 an argument based on the extent of the autocorrelation function is used to give the condition that oversampling the diffraction pattern of an isolated structure by a factor of 2 in each dimension is sufficient. Thus, a support of at most one-half of each dimension is required. This approach has been used successfully for a number of different objects[8,9] but in each case the object was isolated.

II. WAVELET DOMAIN CONSTRAINTS

Although much success has been achieved with the finite support constraint, several reasons motivate exploring other types of constraint sets particularly for specific applications.

(1) The finite support constraint restricts the method to reconstructing isolated objects. Many applications would benefit from being able to image extended structures.
(2) It is often that more detailed spatial information such as low-resolution scanning electron microscope (SEM) or x-ray transmission images may be available. Existing algorithms frequently use this to fill in data values that are missing due to a beamstop.[2]
(3) Rather than precise knowledge of the support, the prior information may be more qualitative in nature. For example, it may be that the structure is semiregular or that it is generally composed of a small number of homogeneous areas.

In this work, we introduce the use of a low-resolution version of the real space object as *a priori* information. It is explicitly not assumed that the sample is compactly supported as previously required. The constraint set is now the set of all images that have a low-resolution approximation matching the measured values. It is expected that the resolution could be lower by perhaps a factor of 16 or 32.

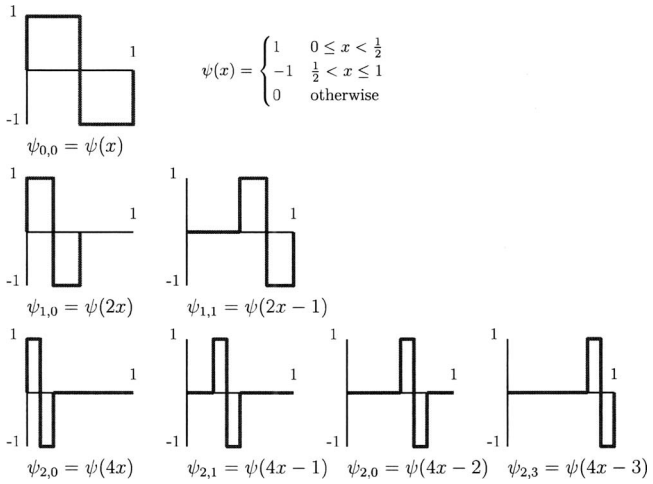

FIG. 2. Several of the continuous Haar wavelets. The mother wavelet $\psi(x)$ is scaled and shifted.

These *a priori* data directly provide information about the low frequency components in the Fourier domain, both the phase and magnitude. The magnitude information can prove useful as a beamstop generally obscures the center portion of the image sensor. The low-resolution information sets the approximate structure of the object and resolves phase and translation ambiguities.

The low-resolution constraint may be applied in the spatial domain but can be more readily expressed in a wavelet domain. For an excellent introduction and reference to wavelets and their uses see Ref. 10. The Haar wavelet is suitable partly not only because of its simplicity but also because the structure of the wavelet matches the shape of the expected features the test sample. For other sample types, one of the other wavelets may be more suitable. Figure 2 shows the continuous Haar mother wavelet and several translated and scaled wavelets. Figure 3 illustrates the wavelet decomposition of a two-dimensional image. For the Haar wavelet a single level of decomposition produces four smaller images ($\frac{1}{2}$ the size in each dimension). The first image is the (normalized) approximation subimage where the sum of each 2 $\times$2 block is computed. The second, third, and fourth images are detail subimages where the difference between sample values horizontally, vertically, and diagonally are computed. Additional levels of decomposition can be recursively performed on the sum image. In Fig. 3 four levels of decomposition are shown with the shaded block indicating the approximation coefficients that will be used as *a priori* information.

It is assumed that the diffraction data are of size $(n \times n)$ for some $n=2^k$, where k is a positive integer and that the low-resolution information is of size $(2^l \times 2^l)$, where l is also a positive integer and $l<k$. The approximation coefficients of the $(k-l)$th wavelet transform, $\mathcal{W}_{k-l}$, are then constrained to match the *a priori* information in wavelet space X_W^{meas}.

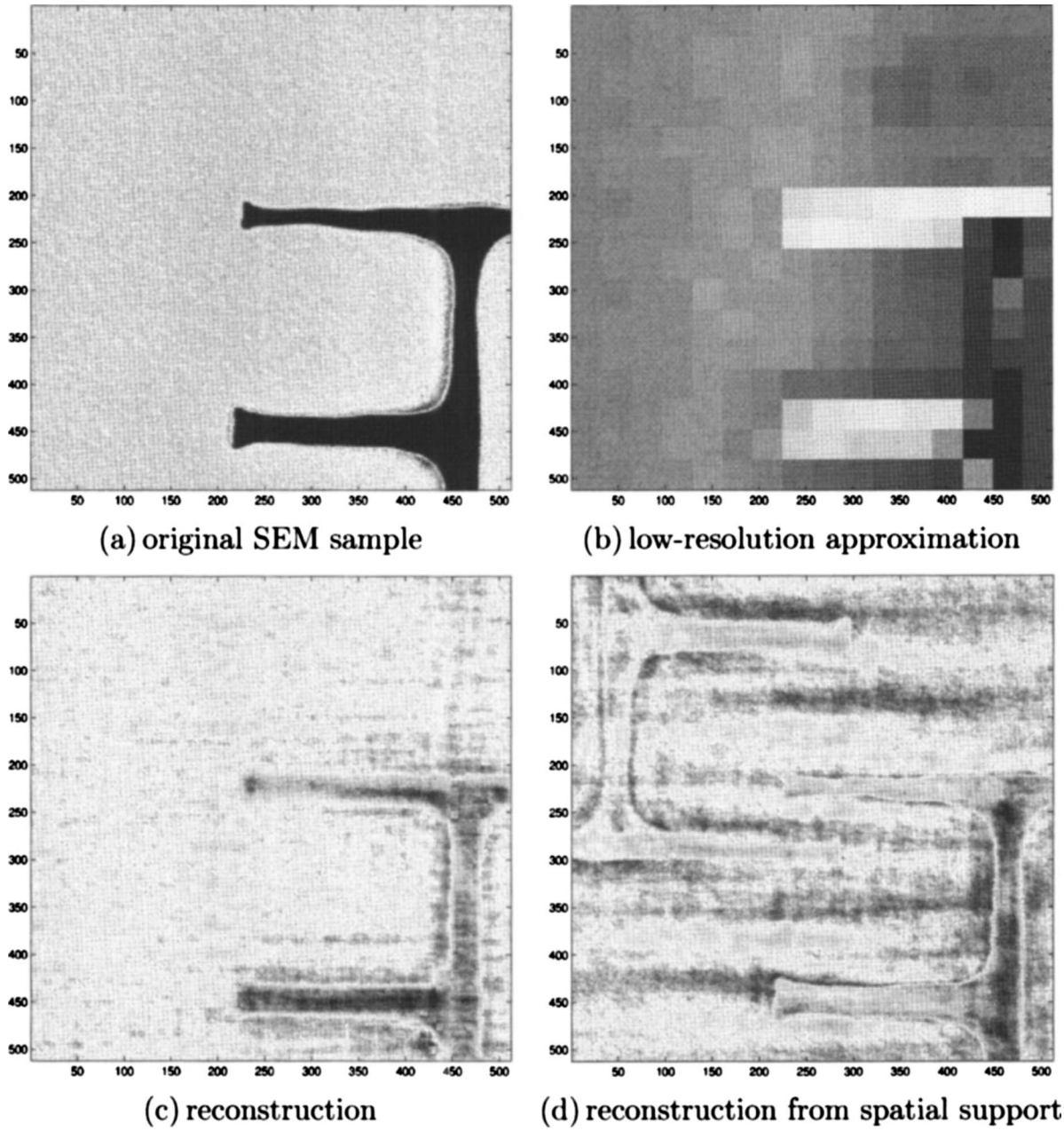

FIG. 4. Iterative phase reconstruction where constraints are enforced in the Fourier domain and in the wavelet domain. (a) shows the original sample from which diffraction measurements are obtained, (b) shows the low-resolution approximation used for the wavelet constraint, (c) shows the reconstruction using constraints in wavelet space, while (d) shows a reconstruction using a basic finite support constraint (the support is not modified as the algorithm progresses—as such, the phase ambiguity is not resolved).

Figure 3 shows the approximation coefficients for the fourth level decomposition. The constraint set is

$$B^w = \{x | [\mathcal{W}_{k-l}(x)]^{\text{approx}} = X_W^{\text{meas}}\}. \tag{11}$$

The orthogonal projection is obtained by performing the $(k-l)$ level wavelet transform, setting the approximation coefficients to the low-resolution measurements, and then performing the inverse wavelet transform

$$P_{B^w} = \mathcal{W}_{k-l}^{-1}([\mathcal{W}_{k-l}(x)]^{\text{detail}}, [X_W^{\text{meas approx}}]). \tag{12}$$

Because the orthogonal projection sets the low-resolution approximation coefficients, the change in the value is uniformly distributed over all of the sample points which contribute to each coefficient. This leads to the adjustment being performed on blocks of size 2^{k-l} in the projected iteration. This leads to artificial discontinuities between blocks which can be greatly reduced by distributing the required change to values in a smooth nonuniform way across all of the sample points. A nonorthogonal projection can be defined as

$$\overline{P_{B^w}} = x + \gamma, \tag{13}$$

where γ is the solution of the following optimization problem;

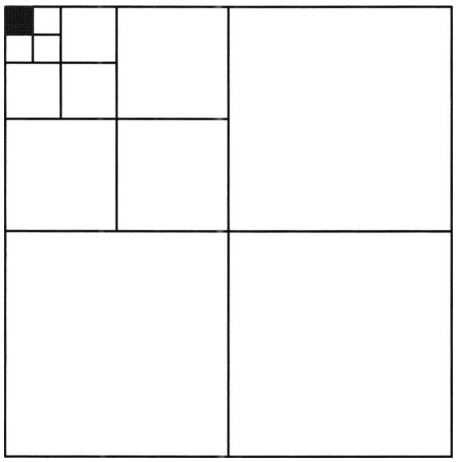

FIG. 3. Image is decomposed to the kth level using the discrete wavelet transform. The unshaded areas are the detailed coefficients at each level. The *a priori* knowledge constrains the shaded approximation coefficients at level k (in this example $k=4$).

$$\text{minimize} \quad \|\mathcal{W}_{k-l}(\gamma) - X_W^{\text{meas}}\|_2 + \|\delta_{\text{vert}}\|_2 + \|\delta_{\text{horiz}}\|_2, \qquad (14)$$

where $\|\cdot\|_2$ is the l^2 norm and δ_{vert} and δ_{horiz} are the difference vectors formed by the pairwise differences of adjacent sample values in the vertical and horizontal directions respectively. The solution of the minimization problem has low-resolution coefficients that match the known data (from the first term) and is smooth in both the vertical and horizontal directions (the second and third terms).

III. RESULTS

Simulation was used to validate that the low-resolution image provided sufficient information for reconstruction. The quality of the reconstruction was also compared to a reconstruction using the HIO algorithm,[3] although the focus of this work is to show the feasibility of reconstruction rather than to compare the quality.

The SEM image of Fig. 4(a) was assumed as the exit surface wave of the diffracting object. The image values were real and positive. This wave was propagated into the far field by the discrete Fourier transform. The amplitudes of the Fourier coefficients were retained and used as the simulated diffraction measurement data for both reconstruction algorithms.

The low-resolution data to be used as *a priori* information, shown in Fig. 4(b), was obtained by first transforming the SEM image of Fig. 4(a) to the wavelet domain with four levels of decomposition. All of the detail coefficients were then set to zero and the image was reconstructed. This has the effect of replacing each 16×16 block of the original image with the average of the block.

The low-resolution information in Fig. 4(b) was used in the wavelet constraint and projection of Eq. (12). Figure 4(c) shows the reconstruction after 500 iterations. The successful reconstruction illustrates that even without a finite support, the low-resolution information is sufficient. For comparison, Fig. 4(d) shows the result of 500 iterations of the hybrid input-output algorithm where the same diffraction data were used with the minimal rectangular support which covered the structure. The support was not refined over time with a dynamic support such as the "shrink wrap" algorithm.[11] The second copy of the structure is due to a phase ambiguity. In both cases the algorithms were initialized with random phases and both reliably converged to the results as shown across many initializations.

IV. DISCUSSION

The purpose of this work has been to report that low-resolution sample information is indeed sufficient to allow reconstruction from Fourier magnitude data. This indicates that it may be worthwhile to examine a range of different possible constraints to augment or supplant the existing widespread use of a finite spatial support constraint. These early results are qualitative only and no direct quantitative comparison to the existing reconstruction methods has been performed. This is the subject of an ongoing research.

V. CONCLUSION

In this work, we have demonstrated a successful reconstruction from simulated diffraction without requiring a finite spatial support. Additional information in the form of a low-resolution image of the diffracting sample was used. This information formed a second constraint space, which was expressed in the Haar wavelet domain. A suitable projection operator was given such that the framework of the difference map algorithm could be applied to reconstruct the sample. The reconstruction was successful and qualitatively was similar to the reconstruction from the well-studied HIO algorithm.

ACKNOWLEDGMENTS

This work was partially supported by DARPA TRUST Program, Applied Material Fellowship, and Texas Instruments. Additionally, the authors would like to acknowledge helpful discussions and comments from Pierre Thibault. One of the authors (Ali Rad) was working with the Peace Group, Center for Integrated Systems, Stanford University, under a summer research collaboration.

[1] J. R. Fienup, J. Opt. Soc. Am. A **4**, 118 (1987).
[2] J. Miao, P. Charalambous, J. Kirz, and D. Sayre, Nature (London) **400**, 342–344 (1999).
[3] J. R. Fienup, Appl. Opt. **21**, 2758 (1982).
[4] V. Elser, J. Opt. Soc. Am. **20**, 40 (2003).
[5] V. Elser, I. Rankenburg, and P. Thibault, Proc. Natl. Acad. Sci. U.S.A. **104**, 418 (2007).
[6] P. Thibault, V. Elser, C. Jacobsen, D. Shapiro, and D. Sayre, Acta Crystallogr., Sect. A: Found. Crystallogr. **62**, 248 (2006).
[7] J. Miao, D. Sayre, and H. N. Chapman, J. Opt. Soc. Am. A **15**, 1662 (1998).
[8] D. Shapiro *et al.*, Proc. Natl. Acad. Sci. U.S.A. **102**, 15343 (2005).
[9] Q. Shen, I. Bazarov, and P. Thibault, J. Synchrotron Radiat. **11**, 432 (2004).
[10] S. Mallat, *A Wavelet Tour of Signal Processing, The Sparse Way* (Academic Press, Burlington, MA, 2008).
[11] S. Marchesini, H. He, H. N. Chapman, S. P. Hau-Riege, A. Noy, M. R. Howells, U. Weierstall, and J. C. H. Spence, Phys. Rev. B **68**, 140101 (2003).